

Theoretical Study of Electronic Properties of Zintl Phase KSi

L. H. Yang,[†] Charles D. Consorte,[‡] C. Y. Fong,^{*,‡} J. E. Pask,[‡] E. Nabighian,[‡]
Susan M. Kauzlarich,[§] and J. S. Nelson^{||}

*H Division, Lawrence Livermore National Laboratory, Livermore, California 94551,
Department of Physics and Department of Chemistry, University of California,
Davis, California 95616, and Semiconductor Material and Device Sciences Department, 1113,
Sandia National Laboratories, Albuquerque, New Mexico 87185*

Received June 26, 1998. Revised Manuscript Received October 16, 1998

We have studied the electronic properties of Zintl phase KSi, by the ab initio density functional pseudopotential method. Our interest in this Zintl compound is in its current use as a reagent in the synthesis of Si nanoclusters. The structure consists of isolated Si₄ tetrahedra with K atoms situated above each face. The crystal system is cubic with the symmetry of the *P43m* space group. Band structure calculations show a band gap of 1.3 eV. The presence of K atoms has widened the band gap over that found between occupied and unoccupied energy levels in the Si₄ cluster. The valence bandwidth lies between the valence bandwidth of crystalline Si with diamond structure and the width of the occupied energy levels of the Si₄ cluster. The density of states shows four major structures for the occupied bands. The lowest energy band of conduction states is also given in the density of states plot. The nature of the bonding in the crystal is revealed by an examination of the charge density associated with each of the structures in the density of states. It is found that the dominant bonding between Si atoms is not the covalent bonding of sp³ hybridized orbitals, as found in diamond structure Si, but is rather a mutual overlap of s- and p-like mixed atomic states from each Si atom. These overlapped states form a bonding state located at the center of the tetrahedron. Furthermore, each K atom is ionized by the nearest Si₄ tetrahedra, allowing the Si atom to fill its 3s and 3p shells.

I. Introduction

One active area of research in device applications is the effective growth of nanoparticles, especially silicon (Si) nanoparticles. Because of the visible luminescence seen in porous Si,¹ the prospect of Si nanoparticles possessing useful optoelectronic properties has generated great interest in possible applications. To date, three popular methods have been devised to produce Si nanoparticles. The most popular method is the gas-phase decomposition of silanes.^{2–4} The second method is the ultrasonic dispersion of porous Si in various solvents to produce colloidal suspensions of Si nanoparticles.^{5,6} However, both of these methods produce a large distribution of sizes and neither allows for control over the surface capping of the clusters. The third method is a solution-phase synthesis of Si nanoparticles using the Zintl salt KSi as a starting reagent. This method

has the potential to yield large quantities of Si nanoparticles.⁷

Zintl phases exhibit many unusual bonding features, structural configurations, and oxidation states.⁸ They are made up of electropositive alkali or alkaline earth elements and electronegative main group elements. The electropositive element donates its electron(s) to the main group element which uses the electron(s) in the formation of bonds to satisfy valence. Typically, Zintl phases show both ionic bonding, between the electropositive and electronegative elements, and covalent bonding, as homoatomic clusters or networks. Corbett⁹ gives an overview of bonding rules for Zintl anions. Zintl phases were shown to be useful for the synthesis of novel cluster complexes as early as 1977.^{8,10} The structure of KSi has been known since 1961¹¹ but there are only a few examples of its use as a reagent.^{7,12–14}

[†] Lawrence Livermore National Laboratory.

[‡] Department of Physics, University of California.

[§] Department of Chemistry, University of California.

^{||} Sandia National Laboratories.

(1) Canham, L. T. *Appl. Phys. Lett.* **1990**, *57*, 1046.

(2) Littau, K. A.; Szajowshki, P. J.; Muller, J. A.; Kortan, A. R.; Brus, L. E. *J. Phys. Chem.* **1993**, *97*, 1224.

(3) Zhang, D.; Kolbas, R. M.; Mehta, P.; Singh, A. K.; Lichtenwalner, D. J.; Hsieh, K. Y.; Kingon, A. I. *Mater. Res. Soc. Symp. Proc.* **1992**, *35*, 1992.

(4) Fojtik, A.; Henglein, A. *Chem. Phys. Lett.* **1994**, *221*, 363.

(5) Heinrich, J. L.; Curtis, C. L.; Credo, G. M.; Kavanagh, K. L.; Sailor, M. J. *Science* **1992**, *255*, 66.

(6) Bley, R. A.; Kauzlarich, S. M.; Davis, J. E.; Lee, H. W. H. *Chem. Mater.* **1996**, *8*, 1881.

(7) Bley, R. A.; Kauzlarich, S. M. *J. Am. Chem. Soc.* **1996**, *118*, 12461.

(8) von Schnering, H. G. *Angew. Chem., Int. Ed. Engl.* **1981**, *20*, 33.

(9) Corbett, J. D. *Struct. Bonding* **1997**, *87*, 157.

(10) *Chemistry, Structure, and Bonding of Zintl Phases and Ions*; Kauzlarich, S. M., Ed.; VCH: New York, 1996.

(11) Busmann, E. *Z. fur Anorg. Allg. Chem.* **1961**, *313*, 90.

(12) Bley, R. A.; Kauzlarich, S. M. *Nanoparticles in Solids and Solutions*; Fendler, J. H., Dekany, I., Eds.; Klumer Academic: The Netherlands, 1996; p 467.

(13) Bley, R. A.; Kauzlarich, S. M. *Nanoparticles and Nanostructured Films*; Fendler, J. H., Ed.; Wiley-VCH: New York, 1998; p 101.

(14) Hey-Hawkins, E.; von Schnering, H. G. *Chem. Ber.* **1990**, *124*, 1167.

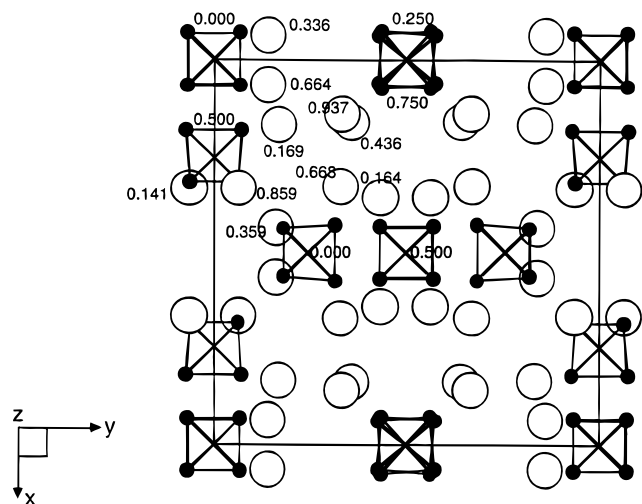


Figure 1. A [001] section showing the atomic configuration of KSi inside a unit cell. The filled and open circles represent the Si and K atoms, respectively. The coordinates are given for those atoms in the upper left corner of the cell (in normalized units. Multiply by 23.84835 a_0 to obtain actual coordinates).

There has been increased interest in the theoretical study of Zintl phases.^{15–23} A review article by van der Lugt²⁰ strives to resolve some discrepancies between experimental and theoretical results. In addition, the electronic properties of KGe, NaGe, and NaSi are examined by Tegze and Hafner.²¹ KSi has been the subject of a theoretical study by Galli and Parrinello;²² however, their interest was in structural studies of molten KSi. Experimentally, KSi has been shown to be among the most promising materials for growing Si nanoparticles for future electronic devices.⁷ It is opportune to investigate the electronic properties of KSi in order to understand the bonding in this phase. From these results, the growth mechanism for Si nanoparticles, using KSi as a reagent reacting with SiCl_4 , can then be inferred or further examined. Therefore, our first step is to understand the electronic properties of Zintl phase KSi by means of ab initio self-consistent pseudopotential¹⁹ calculations.

II. Computational Details

KSi has a simple cubic structure, as shown by Busmann,¹¹ who has given a review of similar structures. The experimental lattice constant is 23.856 a_0 (Bohr units)⁸ and this was used as the starting point for the calculation of the electronic properties. There are 32 Si and 32 K atoms in a periodic unit cell. They are arranged to have the T_d^4 or $P43m$ space group. Figure 1 shows a [001] projection of the unit cell. The small, filled circles indicate Si atoms, while the large, open

circles represent the K atoms. In the upper left corner, the z-coordinates of the K atoms, in fractional units (multiply by the unit cell size of 23.84835 a_0 to obtain actual coordinates), and the center of the Si_4 tetrahedra are indicated near the circles and on top of the cluster, respectively. The Si atoms occur in groups of four, forming tetrahedral clusters. The presence of strongly bonded clusters, embedded in the alkali metal solution, is a typical feature of Zintl phases.

To theoretically determine the equilibrium configuration of the atoms inside a unit cell, there are three types of parameters that need to be optimized in a given unit cell: the electron wave functions, ion positions, and unit cell parameters. Our optimization technique is to minimize the total energy with respect to these parameters.

For the solutions of the electronic wave functions, we solve the Kohn–Sham equations based on the local density approximation (LDA)²⁴ within the framework of density functional theory (DFT)²⁵ using the plane-wave pseudopotential method.¹⁹ We used Perdew and Zunger's²⁶ parametrization of Ceperley and Alder's²⁷ results to approximate the exchange-correlation effects. A preconditioned conjugate gradient technique based on the scheme of Teter et al.²⁸ was developed for efficiently optimizing the electronic wave functions. Soft pseudopotentials of K and Si, constructed within the scheme developed by Troullier and Martins,²⁹ are used. These potentials implement the Kleinman and Bylander³⁰ scheme to render their nonlocal parts separable. The development and the testing of the codes used in this study have been reviewed by Yang.³¹ The K potential was generated using the neutral $4s^1 4p^0 3d^0$ configuration as the reference state with a radial cutoff of 2.75 a_0 for the s component and a radial cutoff of 3.75 a_0 for the p and d components of the potential. The s angular momentum channel was treated as a local component while the p and d angular momentum channels were treated as the nonlocal components of the potential. The Si potential was generated using the $3s^2 3p^2 3d^0$ configuration as a reference state. A single radial cutoff of 1.9 a_0 for the s, p, and d components of the potential was used. The s and p angular momentum channels were treated as nonlocal components, and the d channel was treated as the local component of the potential. Four special \mathbf{k} -points³² in the irreducible part of the first Brillouin zone (BZ) were used to determine the self-consistent potential for this crystal. A cutoff energy of 54 Ry is used, resulting in a total of about 86 000 plane waves for each \mathbf{k} -point. Ionic positions were optimized by calculating the forces acting on the ions in the unit cell with a particular lattice constant after each self-consistent wave function solution and then displacing accordingly.

(15) Cave, R. J.; Davidson, E. R.; Sautet, P.; Canadell, E.; Eisenstein, O. *J. Am. Chem. Soc.* **1989**, *111*, 8105.

(16) Alemany, P.; Alvarez, S.; Hoffmann, R. *Inorg. Chem.* **1990**, *29*, 3070. Sherwood, P.; Hoffmann, R. *J. Am. Chem. Soc.* **1990**, *112*, 2881.

(17) Axe, F. U.; Marynick, D. S. *Inorg. Chem.* **1988**, *27*, 1426.

(18) Tegze, M.; Hafner, J. *Phys. Rev. B* **1989**, *39*, 8263.

(19) Gallup, R. F.; Fong, C. Y.; Kauzlarich, S. M. *Inorg. Chem.* **1992**, *31*, 115.

(20) van der Lugt, W. *J. Phys.: Condens. Matter* **1996**, *8*, 6115

(21) Tegze, M.; Hafner, J. *Phys. Rev. B* **1989**, *40*, 9841

(22) Galli, G.; Parrinello, M. *J. Chem. Phys.* **1991**, *95*, 7504

(23) Nesper, R.; A Currao, Wengert, S. In *Organosilicon Chemistry II*; Auner, N., Weis, J., Eds.; VCH: New York, 1996; p 469.

(24) Kohn, W.; Sham, L. *Phys. Rev.* **1965**, *140*, A1133.

(25) Hohenberg, P.; Kohn, W. *Phys. Rev.* **1964**, *136*, B864.

(26) Perdew, J.; Zunger, A. *Phys. Rev. B* **1981**, *23*, 5048.

(27) Ceperley, D. M.; Alder, B. J. *Phys. Rev. Lett.* **1980**, *45*, 566.

(28) Teter, M. P.; Payne, M. C.; Allen, D. C. *Phys. Rev. B* **1989**, *40*, 12255.

(29) Troullier, N.; Martins, J. L. *Phys. Rev. B* **1989**, *40*, 2980.

(30) Kleinman, L.; Bylander, D. M. *Phys. Rev. Lett.* **1982**, *48*, 1425.

(31) Yang, L. H. Advanced Atomic-level Materials Design in a Massively Parallel Environment. In *Industrial Strength Parallel Computing*; Konigas, A., Ed.; Morgan Kaufmann Publishers: New York, in press.

(32) Monkhorst, H. J.; Pack, J. D. *Phys. Rev. B* **1976**, *13*, 5188.

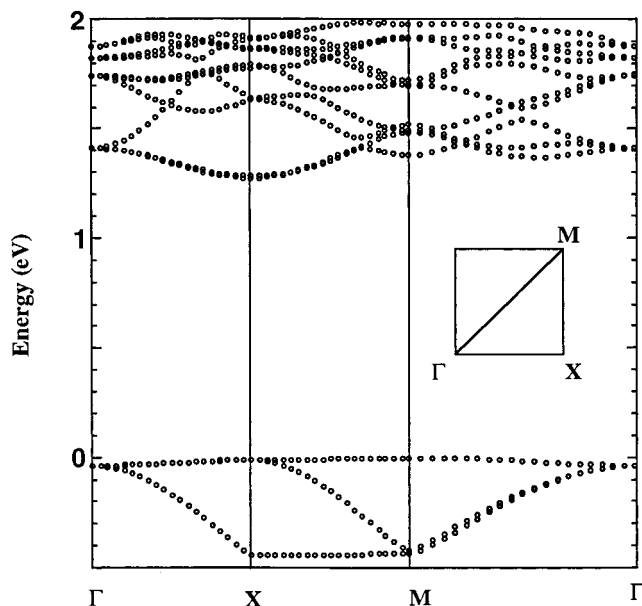


Figure 2. The band structure of KSi near the band gap.

III. Results and Discussion

A. Lattice Structure. The calculated lattice constant is about 1% smaller than the experimental value.⁸ The atomic positions differ from those given in ref 11 by less than 2%.

B. Band Structure. Figure 2 shows the band structure of KSi near the band gap. The dispersion of the occupied bands (variation in energy vs \mathbf{k} in the BZ) is very small mainly due to the weak interaction between Si_4 tetrahedra. The calculated total width of the valence band (VB) is 11.1 eV. The energy difference between the top of the VB and the bottom of the conduction band (CB) is 1.3 eV. This value is expected to be about half of the measured energy gap because LDA-DFT in general underestimates the energy gap for semiconductors and insulators.³³ We note from Figure 2 that this energy gap is indirect, with the highest point in the valence band being at the M point and the lowest point in the conduction band at the X point in the BZ. However, the highest energy valence band is quite flat and the energy difference between the M point and the X point (0.01 eV) is within the uncertainty of these calculations. Our results suggest that KSi is a wide gap semiconductor.

To gain an understanding of the effects of the clustering of the Si atoms in the K solution, we contrast these results with the corresponding DFT-LDA results of pure diamond structure crystalline Si and a single tetrahedral Si_4 cluster. The VB width of KSi lies between the VB width of crystalline Si (12.6 eV)³⁴ and the width of the occupied energy levels for the single Si_4 tetrahedral cluster (10.2 eV). The calculated DFT-LDA energy gap of KSi is larger than that of both crystalline Si (0.5 eV) and the Si_4 tetrahedron (0.4 eV). Presumably this is due to the presence of K atoms in KSi. The comparison of the VB width indicates that the bonding between Si atoms in KSi differs from the covalent bonding present

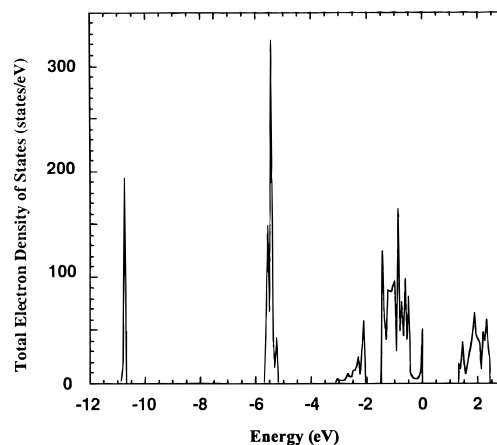


Figure 3. Total occupied density of states.

in crystalline Si and more closely resembles the bonding of a tetrahedral Si_4 cluster. Examining the charge densities provides more conclusive information.

C. Density of States. The density of states (DOS) for the occupied and the lowest energy unoccupied states is calculated using 20 \mathbf{k} -points distributed uniformly in the irreducible part of the first BZ and is shown in Figure 3. The states below the top of the VB (set to 0 eV for reference) are grouped into four bands. The qualitative features of the DOS are similar to those exhibited by other Zintl phases of this structure type.²¹ The lowest energy band of states exhibits a peak at about -11 eV. The next band of states has its peak centered at -5.5 eV. The remaining structures in the DOS are more complex, and assigning a single peak to these structures is difficult. However, we can remark that the highest point of the next structure occurs at -2.1 eV. The states near the band gap split into two structures. One has its highest point at -1.9 eV, and the other has its highest point very near 0 eV. In addition, a high point at 1.8 eV, above the reference, is observed for the lowest band of conducting states. To identify the origin of each structure in the DOS, we calculated the charge densities associated with each band of states in sections of the unit cell.

D. Charge Densities. To identify the bonding nature associated with the different structures in the DOS, a thorough examination of the charge density was done throughout the unit cell for electrons in several different \mathbf{k} -states and having energy in the appropriate range associated with each structure. Since, for each structure in the DOS, the dominant physical features of the charge density were present for each \mathbf{k} -point, we present only the results of the Γ ($\mathbf{k}=0$) point.

Since the unit cell has the simple cubic structure and the atoms are symmetrically located (aside from a slight relaxation) with respect to the center of the unit cell, the following charge density plots are all planes that are parallel to the x - y plane. In most plots, we will be focusing our attention on the central Si_4 tetrahedron. The z -coordinate of the plane is shown and was chosen to best display the dominant features of the charge density within the energy range shown.

The darker areas of the plots represent regions of high charge density and the atoms are labeled when they are within $1 a_0$ of the plane and labeled in bold when they are within $0.1 a_0$ of the plane.

(33) Sham, L. J.; Schluter, M. *Phys. Rev. Lett.* **1983**, *51*, 1888.

(34) Papaconstantopoulos, D. A. *Handbook of the Band Structure of Elemental Solids*; Plenum Press: New York, 1986, p 234.

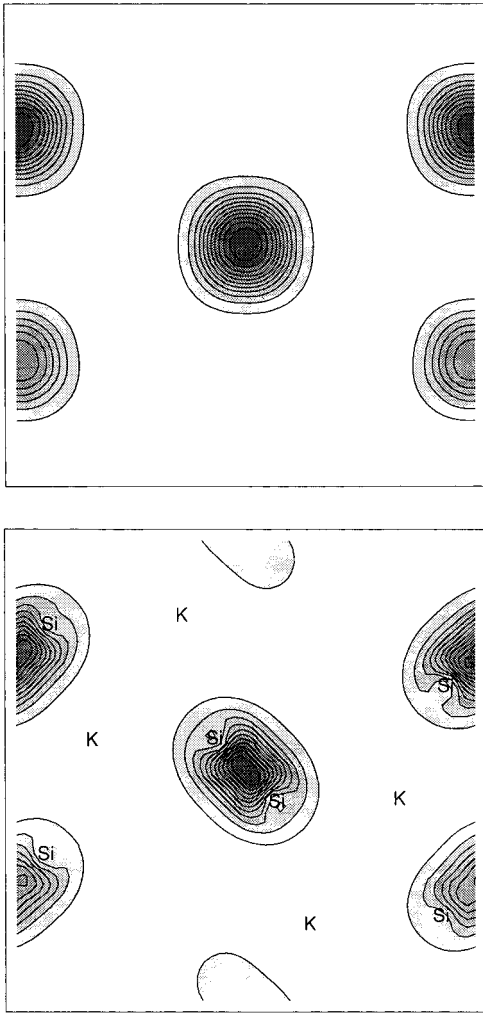


Figure 4. (a) The charge distribution in the (001) section at $z = 11.924 a_0$ for the $\mathbf{k} = 0$ state within the -12 to -10 eV energy range of the DOS. (b) The charge distribution in the (001) section at $z = 9.424 a_0$ for the $\mathbf{k} = 0$ state within the -12 to -10 eV energy range of the DOS.

In Figure 4, we show the charge density associated with the lowest energy structure in the DOS. Figure 4a shows the $z = 11.92 a_0$ slice (center of the unit cell) and Figure 4b shows the $z = 9.42 a_0$ slice. The main feature of this structure is that the charge is contained almost entirely within the Si_4 tetrahedra. However, the maximum charge density ($2.95 e/a_0^3$) is located in the center of the cluster and not between the Si atoms ($0.85 e/a_0^3$). This implies that the Si atoms are bonded together not through the covalent bonding of sp^3 hybridized orbitals, as in diamond structure crystalline Si, but through a mutual overlap of mixed s- and p-like atomic orbitals from each of the four Si atoms. Each atom shares three electrons through the overlap. Also of interest is the complete lack of charge around the K atoms. In fact, none of the structures in the DOS below the top of the valence band show any charge associated with the K atoms.

The interesting feature of the next peak in the DOS is the localization of charge around the Si atoms as shown in the $z = 10.42 a_0$ slice of Figure 5. The fact that the charge is spherically distributed and that there is minimal charge between the atoms suggest that the orbitals have retained much of their atomic s-like

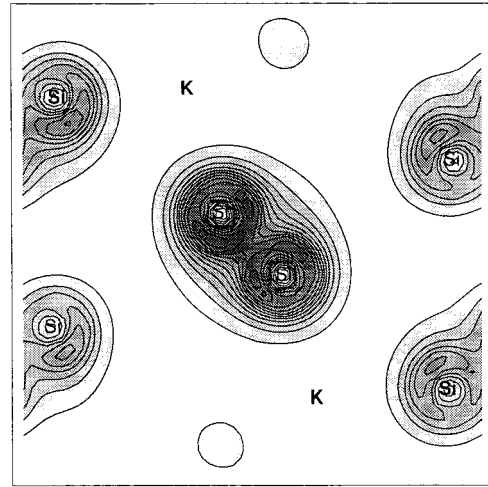


Figure 5. The charge distribution in the (001) section at $z = 10.424 a_0$ for the $\mathbf{k} = 0$ state within the -7 to -5 eV energy range of the DOS.

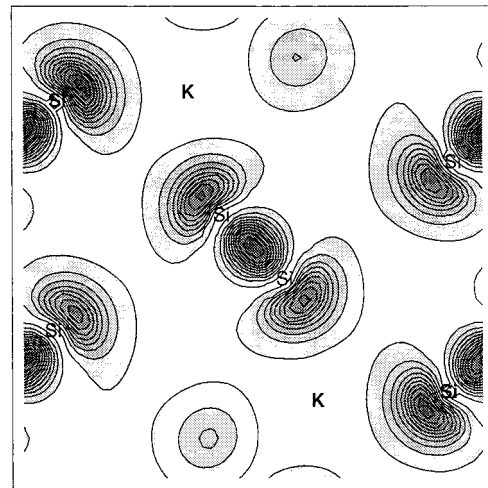


Figure 6. The charge distribution in the (001) section at $z = 10.424 a_0$ for the $\mathbf{k} = 0$ state within the -4 to -2 eV energy range of the DOS.

character. Although it is not shown, it should be pointed out that there is a charge minimum at the center of the Si_4 tetrahedra.

The next structure in the DOS again has its maximum charge density in the center of the Si_4 tetrahedra ($1.7 e/a_0^3$ compared to $0.74 e/a_0^3$ between the Si atoms). However, as seen in the $z = 10.42 a_0$ slice of Figure 6, there is also a considerable amount of charge outside the cluster and a node on each of the Si atoms. Thus the Si clusters exhibit another four-way mutual overlap, but for this energy range, the atomic orbitals are predominantly p in character.

The charge density corresponding to the final structure in the DOS below the top of the valence band is shown in Figure 7. We again show the $z = 11.92 a_0$ slice in Figure 7a and the $z = 10.42 a_0$ slice in Figure 7b. Here, another charge minimum exists at the center of the Si cluster with minimal charge appearing between the Si atoms as well. However, there are now strong charge lobes outside the cluster (the maximum density is $0.74 e/a_0^3$) again with apparent nodes at the Si atoms.

In Figure 8, we show the charge distribution of the $z = 7.92 a_0$ slice for the structure in the DOS that is in

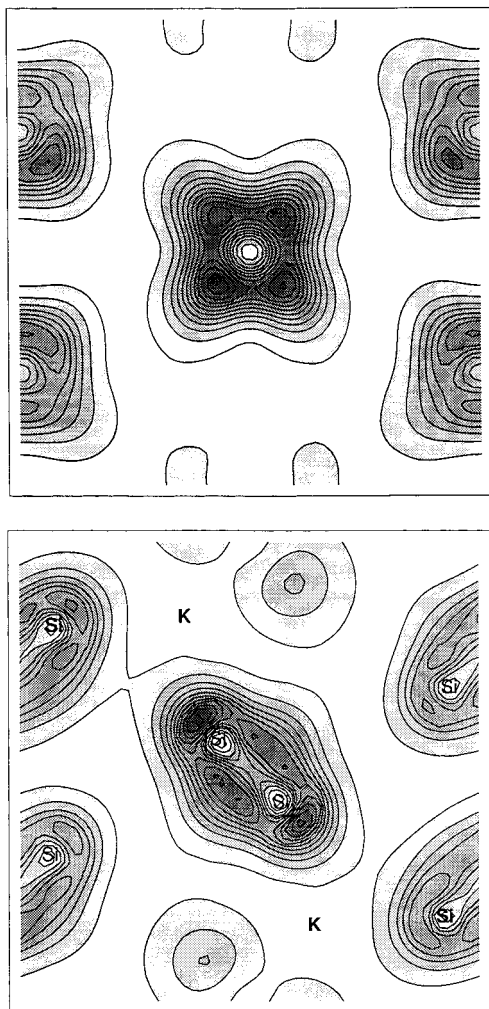


Figure 7. (a) The charge distribution in the (001) section at $z = 11.924 a_0$ for the $\mathbf{k} = 0$ state within the -2 to 0 eV energy range of the DOS. (b) The charge distribution in the (001) section at $z = 10.424 a_0$ for the $\mathbf{k} = 0$ state within the -2 to 0 eV energy range of the DOS.

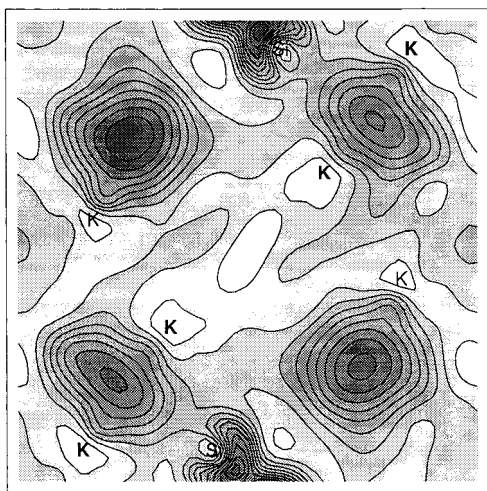


Figure 8. The charge distribution in the (001) section at $z = 7.924 a_0$ for the $\mathbf{k} = 0$ conduction state that exists in the 0 – 2.3 eV energy range of the DOS.

the conduction band. Here, although the charge distribution is more uniform throughout the plane, a common feature for the conduction band, it should be noted that there is a significant concentration of charge between

the nearest neighbor K atoms rather than around each individual K atom. Careful examination has revealed that this charge distribution serves to link Si_4 tetrahedra together and provides conducting channels for an electron excited to the conduction band.

A general picture of the bonding in KSi emerges from the above results: each of the four Si atoms in a tetrahedral cluster shares three of its four valence electrons with its neighbors. This sharing is in the form of mutual overlap of mixed atomic orbitals forming a four-centered bond. This is consistent with calculations of a simple tetrahedral cluster. Furthermore, because there is no charge associated with the K atoms for all DOS structures with energy below the top of the valence band, it appears that the $4s$ electrons from the K atoms are ionized by the Si_4 tetrahedra. Since there are four K atoms per Si cluster, each Si atom now has a completely filled $3p$ subshell. This ionic feature serves to widen the band gap. The structure is therefore held together by ionic bonds between the K atoms and the Si clusters. This is consistent with Zintl–Klemm’s electron-counting rules.^{8–10,23}

IV. Summary

We have applied the ab initio pseudopotential method to study the electronic properties of Zintl phase KSi as the first step in our study of the growth of Si nanoparticles.

While the bandwidth of the occupied states is narrower than that for diamond structure crystalline Si and wider than the width of the occupied energy levels of a single Si_4 tetrahedral cluster, the calculated energy gap is larger than both the crystalline Si gap and the gap between the highest occupied and lowest unoccupied levels of a single Si_4 cluster.

Within the 64-atom unit cell, there are eight four-atom Si tetrahedra, each of which is surrounded by four K atoms. The nature of the bonding between the Si atoms within a tetrahedron is that of a mutual overlap of mixed atomic orbitals that form a bond in the center of each Si cluster. Because one of the lower energy structures in the DOS retains its s character in a nonbonding manner, it is thought that each Si atom shares three of its valence electrons with its three nearest neighbors. Furthermore, the complete ionization of the $4s$ electrons from the four neighboring K atoms by the Si cluster provides the necessary charge for each Si atom in the cluster to complete its $3s$ and $3p$ subshells. This serves to widen the energy gap over that of crystalline Si and makes KSi a wide-gap semiconductor. The charge distribution for the lowest energy structure in the conduction band of the DOS shows the presence of conduction channels. These channels are formed by the sharing of charge between neighboring K atoms and suggest that the crystal should be a good conductor once electrons are excited into the conduction band, making KSi a good candidate for doping.

Acknowledgment. Work at UC Davis was supported in part by the Campus Laboratory Collaboration grant from the University of California. L.H.Y. was supported by the US DOE under contract W-7405-ENG-48. J.S.N. was supported by the US DOE, Office of Energy Research under contract DE-AC04-76P00789.